Scilight

Renewable Chemistry

https://www.sciltp.com/journals/rc

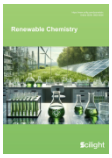

Article

A New Route to Monhydroxycyrene

Majed Almuqhim [1], Con R. McElroy [1,2,*], Jiajun Fan [1] and James H. Clark [1]

[1] Green Chemistry Centre of Excellence, Department of Chemistry, University of York, Heslington, York YO10 5DD, UK
[2] Department of Chemistry, School of Natural Sciences, University of Lincoln, Lincoln LN6 7DL, UK
* Correspondence: CMcElroy@lincoln.ac.uk

How To Cite: Almuqhim, M.; McElroy, C.R.; Fan, J.; et al. A New Route to Monhydroxycyrene. *Renewable Chemistry* **2025**, *1*(1), 3.

Received: 8 April 2025
Revised: 8 July 2025
Accepted: 23 July 2025
Published: 4 August 2025

Abstract: The importance of levoglucosenone (LGO) as a bio-derived platform molecule has been significantly elevated through its transformation into Cyrene™, a widely adopted green solvent. In this study, we investigate the interactions of LGO with water, a key component of biorefinery systems, revealing a new, efficient route to monohydroxycyrene (MHC). This transformation involves the slow, aqueous-based conversion of LGO to a triol intermediate, followed by selective dehydration to form MHC—a chiral molecule with dual functional groups and promising synthetic potential. MHC was synthesised in two simple and green steps without the need for catalysts or reagents, achieving an 88% yield and 98% purity under mild conditions. This environmentally benign approach aligns with the principles of green chemistry by eliminating the need for hazardous reagents and employing water as a sustainable solvent. The structure of MHC was confirmed using a combination of NMR, IR, UV-Vis, CHN, MS, and thermal analyses. Our results also highlight the role of temperature in influencing product formation, with lower temperatures (45–65 °C) enhancing yield, while higher temperatures (e.g., 95 °C) reduce conversion efficiency. MHC exhibits favourable physical and chemical properties, including polarity, solubility, and thermal stability, making it a promising candidate for future applications in green chemistry, pharmaceuticals, and materials science. The combined reactivity of the carbonyl and hydroxyl groups makes MHC a promissing platform molecule for synthesising polymers, pharmaceuticals, and advanced bio-based materials. Moreover, the mild reaction conditions and catalyst-free nature of the process contribute to reduced energy input and lower environmental impact. This work offers new insights into sustainable chemical pathways and provides a strong foundation for scaling up the production of novel biomass-derived building blocks.

Keywords: bio-derived; platform molecule; levoglucosenone

1. Introduction

The Paris Climate Agreement signed in 2015 committed hundreds of countries to achieve Net Zero carbon emissions by 2050, with individual national targets then declared as part of this roadmap [1]. This ambitious global framework aims to limit the rise in average global temperature to well below 2 °C above pre-industrial levels, ideally capping it at 1.50 °C, in order to avoid the most catastrophic impacts of climate change. To achieve these goals, much focus has been placed on power generation and the electrification of transport. These areas have seen rapid technological innovation, investment, and policy support, leading to notable progress in renewable energy deployment [2] and electric vehicle adoption [3]. Another key sector is the chemical industry, which currently accounts for 5% of global emissions [4]. Decarbonising the energy mix is part of the solution, but chemistry intrinsically relies on carbon within its build blocks and as such, Net Zero also includes defossilisation of feedstocks [5]. This calls for a fundamental rethinking of raw material inputs, shifting away from fossil sources

toward renewable alternatives that still meet performance and cost demands. Alongside recycling, CO_2 and green hydrogen, chemicals from biomass are key to realising this goal [6]. The most desirable feedstocks for chemicals from biomass are those previously thought of as wastes [7]. By valorising these waste streams [8], such as agricultural residues [9], forestry by-products [10], or even food [11] and municipal waste [12], the circular economy model can be advanced while contributing to carbon neutrality [13].

Biomass derived platform molecules have been well studied and continue to attract significant research interest due to their potential to replace fossil-based chemicals i.e., a route to defossilisation [14,15]. There are numerous examples of interesting functional compounds that can be obtained in 3 steps or less from renewable biomass resources. These include furfural [16], levulinic acid [17], glycidol [18], itaconic acid [19] and several other key intermediates with broad applicability. Another good example is levoglucosenone (LGO), a bio-based platform molecule, as an alternative for fossil-fuel-based feedstocks [20]. Unlike petrochemical building blocks, LGO is a highly functionalised chiral molecule, which allows the synthesise of a wide range of chemicals including nucleosides [21], anticancer drugs [22], pharmaceutical intermediates [23] and green solvents [24]. Clark et al. produced LGO from unconverted saccharides in waste lignin which is a new perspective in bio-refining, offering a new and resource-efficient perspective on biomass valorisation within the biorefinery framework [25]. Huang et al. on the other hand, produced LGO from levoglucosan (LGA) in the presence of water and an amberlyst catalyst [26]. Most significantly, LGO is produced at scale using the Furacell™ process, a thermochemical method that enhances yield and efficiency, making large-scale production both viable and economically attractive [27].

The importance of LGO as a biomass derived platform molecule has been significantly enhanced by the discovery and commercialisation of its derivative, dihydrolevoglucosenone (Cyrene™) [24]. This transformation underscores the versatility and utility of LGO, not only as a precursor but also as a bridge between traditional biomass and high-value green chemicals. Cyrene™ is proving to be a very successful solvent often as a replacement for toxic NMP and other dipolar aprotic amides [28–30]. Its environmentally benign nature, coupled with comparable solvency power, makes it a preferred choice in various industrial applications including pharmaceuticals, polymer processing, and electronics manufacturing. It is expected to be manufactured on kT scale as described in the EU ReSolute project [31]. Such large-scale production capacity signals a major shift towards more sustainable solvents in the global chemical supply chain. This will be an excellent example of a kiloton second generation biorefinery [27]. Water is ubiquitous in biorefineries and there are a scattering or reports of the reaction of water with LGO and Cyrene notably the reversible formation of a diol and the significance of this on the behaviour of Cyrene as a solvent. Understanding this interaction is critical, as it may influence solvent stability, reactivity, and recyclability, all of which are crucial parameters in green process design.

With the real need for bio-based chemicals as alternatives to those derived from fossil fuel [6,32], simple derivatives of LGO and Cyrene have the potential of being bio-based building block chemicals [33,34]. The drive toward sustainability is fuelling innovation in platform molecules, particularly those that can be readily modified to serve diverse industrial purposes. 5-Monohydroxycyrene (MHC) is one such compound and has been reported as a possible by-product when producing Cyrene from LGO [35–39]. MHC stands out as a novel and underexplored compound with unique structural and functional attributes. Its fixed chirality, combined with both hydroxyl and ketone functionalities, makes it highly attractive for stereoselective synthesis, green chemistry applications, and as a potential intermediate in the pharmaceutical sector. Despite being mentioned as a minor by-product during Cyrene production, MHC has not yet been studied in detail, representing an opportunity to expand the scope of biomass-derived platform molecules. Its formation during Cyrene synthesis highlights the interconnectedness of biomass-derived pathways and the importance of valorising all resulting products, including minor ones [35–37,40]. It can be obtained in two simple and green steps from biomass. These steps follow key principles of green chemistry, including the exclusive use of water as a benign solvent, a catalyst-free conversion process, and operation under mild temperature conditions, which together reduce energy input and eliminate the need for hazardous reagents. The single hydroxyl group in this compound will allow for additional functionalisation providing an easy route to a number of interesting bio-based molecules. This versatility opens doors to tailor-made chemical modifications for specialty chemicals, materials science, or even pharmaceutical applications. As this molecule contains fixed chirality, there is also potential relevance to active pharmaceutical ingredients (APIs) design and could enhance synthesis of the future drug candidates derived from MHC.

2. Results and Discussion

Here we report a thorough investigation of the LGO-water system that shows a key intermediate with an unusually strong hydrogen bond and enabled the isolation and unambiguous structural conformation of MHC. This interaction provides valuable insights into the behaviour of biomass-derived compounds in aqueous environments,

where hydrogen bonding plays a critical role in determining reactivity and stability. In this work, MHC was produced in high yield using simple methods and its structure confirmed with techniques including NMR, IR, UV-Vis spectroscopy, CHN, MS and thermal analysis. The use of these complementary analytical tools provided a comprehensive understanding of the molecular framework and purity of the compound, ensuring robust structural validation. The first step in the routes to MHC involve formation of the triol-LGO as originally reported by Krishna et al. [41] Scheme 1. This intermediate, formed through hydration at both the ketone and alkene, represents a crucial transition state in the conversion pathway and underscores the importance of reaction control for optimal product yield. Some of the properties of MHC are considered and point to potential success for its future as a platform molecule. Its chemical functionality, coupled with its favourable physicochemical characteristics and bio-based origin, positions MHC as a promising candidate for integration into various green chemical applications.

2.1. Synthesis Efficiency

Thermal removal gives the greatest yield of MHC. Both methods of producing MHC shown in Scheme 1 were successful, but hydration followed by thermal removal gave a yield of 88% MHC while solvent extraction in ethyl acetate resulted in only a 45% yield based on GC analysis. This demonstrates that thermal treatment following aqueous conversion is more effective in driving the equilibrium towards the desired product. The purification of the product using column chromatography gave MHC in a purity of 98 and 72%, respectively. The significantly higher yield and purity obtained through the thermal removal pathway suggest its practical scalability and also imply reduction of using solvents. Moreover, the lower efficiency of the ethyl acetate extraction could be attributed to partial solubility issues or incomplete phase separation during the isolation step.

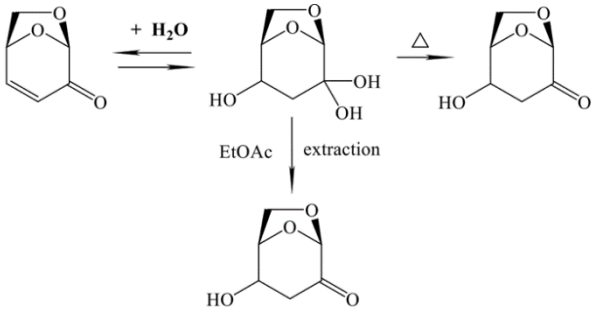

Scheme 1. The two methods of producing MHC by 1. Heating the triol-LGO (to the right) and 2. Using the EtOAc to extract the product (below).

2.2. Previous Synthesis from the Literature

The method described herein is simpler and more sustainable than those previously reported. Diot-Néant et al. [42] produced MHC in 82% yield in the presence of K_3PO_4 at 5 mol%. This was at a 677:1 water to LGO molar ratio carried out at room temperature, with HCl neutralisation and column chromatography work up. Ma et al [36]. Produced MHC from LGO treated with triethylamine (7.9 mol%) in 72% yield. This was at a 555:1 water to LGO molar ratio, at room temperature, with flash chromatography work up Shafizadeh et al. [43] used a similar base initiated protocol with triethylamine 90 mol%, room temperature and a 700:1 water to LGO molar ratio and resulted in 93% yield of MHC. While these methods achieved impressive yields, they all required additional reagents or catalysts, introducing extra steps, complexity, and potential waste streams in the process. Our approach does not require a catalyst (LGO and water only) and occurs at room temperature. This makes the method greener and more economically favourable, especially when considering industrial scalability. The reaction proceeded in two steps, first converting LGO to its associated triol-LGO, followed by dehydration to MHC as shown in Scheme 1. Eliminating the need for elevated temperatures or specialised chemicals not only simplifies the process but also aligns with green chemistry principles.

2.3. Spectral Confirmation of Reaction

Numerous analytical techniques shoed the reaction of the alkene and production of an alcohol. ^{13}C NMR spectroscopic analysis shows the difference between MHC produced from the organic layer extraction before and after purification. The new product MHC has no alkene (loss of peak at 1600 cm^{-1}) and shows a non-conjugated ketone (shift of peak from 1700 to 1750 cm^{-1}) as shown in the Figure S1. This is also confirmed by FTIR, which also shows that the product has no unsaturated CH groups. The IR spectra provide further evidence of structural

integrity by highlighting the carbonyl and hydroxyl vibrations. The products show clear evidence of the presence of the hydroxyl group at 3440 cm^{-1}. MHC undergoes rapid H-D exchange with D_2O with the resulting deuterated product showing a characteristic OD stretch at 2535 cm^{-1}. This behaviour not only confirms the presence of exchangeable protons but also hints at potential applications in isotopic labelling.

2.4. Spectral Characterisation

More intensive analysis confirms the suggested structure of MHC. The ^{13}C NMR spectrum for MHC includes a singlet peak at 77.50 ppm which corresponds to C5 overlapping with the solvent $CDCl_3$ triplet peak: this can be distinguished by DEPT-135 which does not show the quaternary carbon in $CDCl_3$ [35] (see Figure 1). This clear differentiation between the solvent signal and the target carbon peak is critical in ensuring accurate assignment of the carbon framework, especially when working with compounds prone to overlap in the NMR window. ^1H NMR spectrum, Figure S2, shows that the two protons on C3 are in different environments (peaks around 2.4 and 2.8 ppm). Both results of ^1H NMR and ^{13}C NMR match previously reported spectra. These matching results further validate the structural identity and purity of the synthesised compound, reinforcing the success and reproducibility of the synthetic method used.

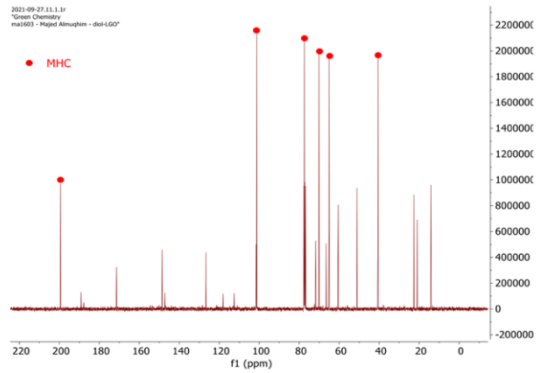

(**A**) MHC before purification

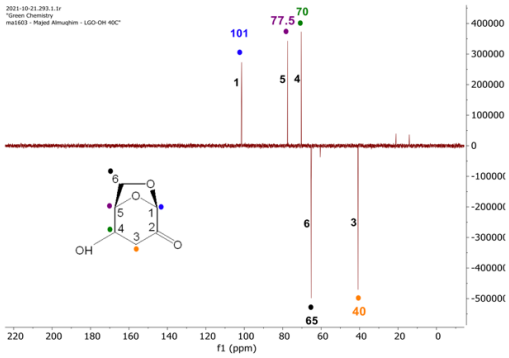

(**C**) DEPT-135 for MHC

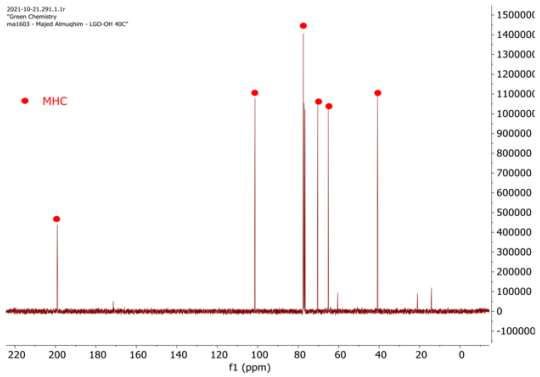

(**B**) MHC after purification

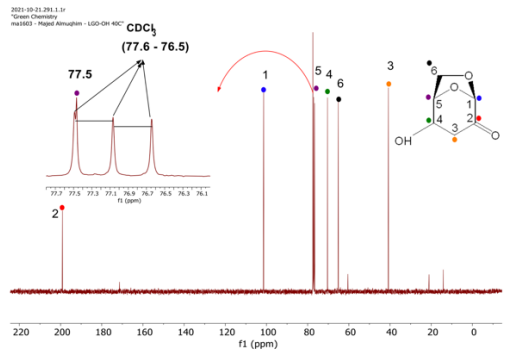

(**D**) ^{13}C NMR for MHC

Figure 1. ^{13}C NMR spectra of MHC; (**A**) showing 6 main bands corresponding to the 6 carbons on the MHC before and (**B**) after purification showing clearer spectrum. (**C**) is DEPT-135 for MHC to deferenciate between CH_2 on C3 and C6 as well as CH on C1, C4 and C5. And lastly (**D**) the spectrum of MHC showing the overlapped band of C5 of the MHC and the solvent $CDCl_3$.

2.5. Reaction with Deuterated Water

In the first method, when LGO was dissolved in D_2O, the D_2O reacts with the alkene to form a new C-H bond as well as the hydroxyl groups as observed clearly by DEPT-135 NMR in (Figure 1) and MS as illustrated in Figure S3 (masses higher by 1 when reacted with deuterium). This observation not only highlights the reactivity of D_2O in exchangeable proton environments but also supporting the formation of hydrated intermediates. Scheme S1 shows the difference between LGO interaction with D_2O and H_2O. Splitting of diastereomer peaks in the 1H NMRs of both D_2O and H_2O products show little control over chirality (peaks around 2.4 and 2.8 ppm) i.e., MHC is obtained as a racemate. This is most likely due to the small size of H_2O/D_2O meaning that the alkene in LGO can be attacked from both above and below as opposed to just the least hindered exo-face [44]. In contrast, previous Michael additions using larger Michael donors show 100% chiral selectivity [45].

MHC shows three different coupling constants of the two protons on the C3 in the range 2.40–2.80 ppm of the ^{1}H NMR spectrum. Using water and deuterium oxide improves our ability to identify the position of each proton in the molecule, and in particular the hydrogen atoms connected to C3 in MHC. The use of D_2O leads to distinct isotopic shifts and allows the assignment of specific hydrogen environments through the observed chemical shift changes and splitting patterns. As shown in Figure S4, a spectrum of MHC prepared from H_2O shows four different bands corresponding to 2 hydrogen atoms boned to C3. This complex splitting pattern could help confirming the molecule's stereochemistry. The molecule may show different coupling constants with the neighbouring atoms bonded to C3. protons that can be calculated as shown in Figures S5 and S14, Tables S5–S8. This data shows a roughly 1:1 ratio of the two isomers based on ^{1}H integration, as well as the C3 protons having 3 coupling constants, 18 Hz with the two non equivalent C3 protons and 1 and 6 Hz between the C4 proton and the two C3 protons.

2.6. Mass Spectrometry

The Mass Spectrometry (MS) analysis (Figure S3 and Scheme S1), confirms the difference of +1 between the two compounds prepared from H_2O and D_2O. The first evident fragmentation for MHC prepared from H_2O has a molecular mass of 116 corresponding to the loss of CO (144 − 116 = 28 CO). This slight mass shift is a direct result of the isotope effect introduced by deuterium, which increases the molecular weight by one unit without significantly altering the chemical behaviour of the compound.

The second fragment has a molecular mass of 98 which corresponds to loss of CO_2 (144 − 98 = 46). Table S1 gives the major fragments of the MHC. Such a loss might help in verifying the structural integrity and molecular framework of the synthesised compound.

The CHN analysis reinforces our confidence in the previous findings. MHC results show that they match MHC theoretical calculations shown in Table S2. The calculated elemental composition based on molecular formula provides a strong secondary confirmation, aligning with spectroscopic evidence and supporting the overall proposed structure of MHC. Accurate CHN results also indicate high product purity and consistency of the synthetic procedure.

2.7. The Effect of the Temperature on MHC Production

Our results suggest that MHC is not stable at high temperatures in the presence of water as some dehydraytion to LGO is observed. Figures S6B, S7 and S8 indicate that the ketone vibration of MHC prepared at 95 °C shows a higher frequency shoulder at (1693 cm^{-1}) compared to lower temperatures. Similarly, the intensity of the major band at 1732 cm^{-1} is slightly lower than the band observed at lower temperatures, indicating a smaller amount of MHC at this temperature. This observation implies a temperature-dependent degradation that becomes more significant under elevated thermal conditions. The shoulder at (1693 cm^{-1}) suggests a conversion of MHC back to LGO that are promoted by heat, particularly in aqueous environments. Although it is very small amount but it suggests a limitation in the thermal processing of MHC-containing formulations and highlights the need for mild processing conditions if MHC is to be preserved in downstream applications.

Although the amount of LGO present in MHC is minimal, the equilibrium of the reaction was affected negatively at higher temperature (95 °C) lowering the amount of MHC produced. As shown in Figures S7 and S8 for the FTIR and ^{13}C NMR spectroscopy there is a noticeable difference compared to the MHC prepared at 95 °C. Temperatures of 45 and 65 °C are better options for the MHC production using the heating method. Increasing the temperature to 95 °C negatively impacts the yield of MHC by promoting dehydration back to LGO. These intermediate temperatures enable higher selectivity for MHC while minimising thermal decomposition or unwanted side reactions. This reverse transformation indicates that excessive heating can drive the equilibrium away from the desired product, especially under conditions where water plays a catalytic or participating role in the reaction. This reverse reaction suggests a shift in equilibrium at high temperature, favouring the reformation of LGO rather than maintaining the MHC product. At lower temperatures it takes much longer for the water to evaporate from the aqueous solution making MHC production more tedious. However, these milder conditions are advantageous when selectivity and preservation of molecular structure are critical, particularly for applications requiring high-purity outputs. Nevertheless, lower thermal stress reduces the by-products of undesired side reactions.

2.8. Polarity Determination

MHC is a highly polar compound. Reichardt's dye was dissolved for a polarity test by dissolving it directly in pure MHC. The solution was analysed using UV-Vis spectroscopy to evaluate solvent polarity. As shown in Figure S9, the dye exhibited an absorption peak at 516 nm which corresponds to the intramolecular charge-transfer $\pi \rightarrow \pi^*$ of the dye molecule. This is specifically related to hydrogen bonding between the OH on MHC and the dye molecule [46], an interaction that does not occur with LGO.

$$E_T\ (30)\ (\text{kcal mol}^{-1}) = 28591/\lambda_{max}\ \text{nm} = 55.40$$

$$E^{N}_{T} = E_T\ (\text{solvent}) - 30.70/32.40 = 0.763$$

The E_T value of the MHC is 55.40 which is high and similar to methanol [36]. The E^{N}_{T} scale ranges from 1.00 for the most polar solvent (water) through to 0.00 to tetramethyl silane TMS as the least polar solvent. MHC has a value of 0.76 which suggests a polar solvent. In comparison, propylene carbonate has an E^{N}_{T} value of 0.47, acetone of 0.36, butanol of 0.59 and ethanol of 0.65 [47]. This indicates how polar MHC is in comparison to a range of aprotic and protic bio-derived solvents.

2.9. Solubility

MHC can be dissolved in many solvents except low polarity ones. It dissolves in water and other polar solvents but not in toluene or hexane. Full tabulated data is available in Table S9. Cyrene, in comparison, dissolves in toluene but not in heptane. This high range of solubility of both Cyrene and MHC highlights the wider range of potential applications. When MHC is dissolved in water, the carbonyl group is attacked very rapidly resulting in formation of the trihydroxy compound. The IR spectrum is illustrated in Figure S10 where no carbonyl signal at around 1700 cm^{-1} is visible. This rapid reaction indicates that the carbonyl in MHC strongly interacts with water. This behaviour is similar to Cyrene. LGO in comparison takes a longer time for the carbonyl to be attacked by the water—the conjugated carbonyl is less reactive. This difference in reactivity is attributable to the LGO's conjugated system, which stabilises the carbonyl and reduces its electrophilicity.

2.10. Dissolving in Water

The MHC which was prepared and dissolved in D_2O was analysed by IR spectroscopy. This experiment aimed to detect how rapidly MHC dissolves and reacts in water. Despite its viscosity, the product easily dissolves by shaking the vial for a few seconds. The solution was then examined by IR spectroscopy.

2.11. Thermal Analysis

The new compound has greater thermal stability than LGO or Cyrene. As expected, the likely strong intermolecular (hydrogen bonding) association in MHC means that it has a higher boiling point than LGO and Cyrene. This suggests that MHC molecules are more tightly held together in the liquid phase, requiring more energy to overcome these cohesive forces during vaporisation. The melting point is below −60 °C which is the minimum temperature that could be reached by the instrument. Both samples of MHC prepared from H_2O and D_2O show similar thermal properties. These are illustrated in Figure S11, with MHC from H_2O showing a differential scanning calorimetry (DSC) phase change peak at 226 °C while the D_2O derived material peak is at 220 °C.

3. Experimental

All samples used in this study were prepared in deionised water at room temperature. Different concentrations for each sample were prepared for quantitative analysis.

Solvents were obtained from Merck or Alfa Aesar, with a typical purity of ≥99%

Circa Group kindly provided the main chemicals, LGO and Cyrene, used in this study. Deionised DI water was provided in-house by the lab using an ELGA CENTRA® system.

3.1. MHC Production Methods

MHC was synthesised from 449.9 g (3.56 mol) of LGO dissolved in 4.5 L (250 mol) of H_2O (70:1 water to LGO molar ratio), forming an aqueous triol-LGO solution (Scheme 1). The reaction proceeded slowly at room temperature, requiring 12 days to reach completion before solvent extraction, and 28 days before rotary evaporation, for full conversion from LGO via the triol-LGO intermediate, as illustrated in Scheme S2. The

resulting triol-LGO was subsequently converted to MHC using two distinct methods, detailed in Scheme 1. The first method involved evaporating the triol-LGO mixture to dryness under reduced pressure using a rotary evaporator at 60 °C for 6 h, inducing ketone formation at C2. As an example, from 1 L of triol solution, almost 120 mL of MHC was obtained. The second method utilised liquid-liquid extraction with ethyl acetate (EtOAc): 200 mL of the aqueous triol solution was transferred to a 1 L separating funnel, and 200 mL of EtOAc was added. Anhydrous magnesium sulfate ($MgSO_4$) was used to dry the organic phase, yielding 15 mL of MHC.

3.2. Thermal Removal

The sample was prepared from LGO (90.67%) dissolved in deuterium oxide (D_2O) at a 10 wt% (error ± 0.14%) loading. Another sample was dissolved in (H_2O) at the same concentration. Both deuterated and non-deuterated samples allowed for a clear comparison between D and H in both IR and NMR spectroscopic techniques for vibrational behaviour and characterisation of MHC respectively. All samples then were evaporated at variable temperatures; 45, 65 and 95 °C. Temperature-controlled evaporation played a significant role in directing the equilibrium influencing the nature and purity of the final product. The ketone was seen to reform from the geminal diol when the water was evaporated.

3.3. Solvent Extraction

10 wt% LGO in water was prepared as described. The sample was stored at room temperature in a sealed vessel for two weeks. This ageing period allowed sufficient time for the slow, spontaneous conversion of LGO to its hydrated form, promoting the natural progression of the reaction without the need for external catalysts or elevated temperatures. 200 ml of the solution was transferred to a separating funnel (1 L) and 200 ml of EtOAc was added. After agitation, the organic layer was removed and dried over magnesium sulphate ($MgSO_4$). This drying step was crucial to remove residual water and avoid reverse hydration during product recovery. The solution was filtered, the ethyl acetate removed under reduced pressure and the product put under high vacuum overnight. This gentle purification approach minimises degradation or loss of volatile components and enhances product stability prior to analysis. See Figure S12 for a visual flow chart.

3.4. IR Spectroscopy

FTIR measurements were carried out using a PerkinElmer Spectrum 400 equipped with an Attenuated Total Reflectance (ATR) accessory, operated at ambient temperature. Each spectrum was acquired with a resolution of 4 cm^{-1} over 16 scans, and a background spectrum of ambient air (16 scans) was subtracted prior to every run. This ensured that all sample spectra were accurately referenced, minimising environmental and instrumental noise. The ATR mode was employed for sampling. This method offers the advantage of minimal sample preparation, allowing for direct analysis of liquids, solids, or gels without the need for dilution or pellet formation. And the spectral data were processed and interpreted using OriginPro 2020b software.

3.5. UV-Vis Spectroscopy

A Jasco V-550 UV-vis spectrometer at a range of 190–900 nm with scanning speed of 1000 nm/min and a band width of 1.00 nm was used. The path length of the cell is 1.00 cm. This standard path length provided a reliable baseline for absorbance measurements, ensuring consistency across all samples. The data was analysed using Spectra Manager software which allowed for precise peak identification and spectral analysis and the data were collected and presented using the OriginPro 2020b software. This enabled advanced plotting and data fitting, facilitating a clearer interpretation of the spectral data.

3.6. NMR Spectroscopy

Three different instruments were used: 300, 400 and 500 MHz NMR spectrometer. All analysis performed at room temperature and $CDCl_3$ as a solvent. The data was analysed using Mnova.

4. Conclusions

Renewable bio-derived platform molecule levoglucosenone (LGO) has been successfully converted to MHC in two simple and green steps using only water without any catalyst or reagent. This environmentally friendly approach aligns with the principles of green chemistry, minimising both waste and the need for hazardous chemicals. MHC was produced in high yield (98%) under mild conditions at room temperature, demonstrating the potential for practical and scalable production in biorefinery sitting. However, it is important to acknowledge that

the conversion process, despite its simplicity, occurs slowly over an extended period—often requiring several days to reach completion. This prolonged reaction time may present limitations for industrial applications where rapid throughput is essential.

The detailed study on MHC in water system revealed that moderate temperatures (approximately 45–70 °C) enhance the formation of MHC, whereas higher temperatures (90 °C) negatively impact the yield. This temperature dependency underscores the need for precise process control to maximise reaction efficiency and ensure consistency. While operating at these intermediate temperatures may reduce energy consumption, balancing conversion speed with thermal efficiency remains a challenge for large-scale implementation.

MHC has been fully characterised using different analytical techniques. The new compound contains a single hydroxyl group that enables intermolecular interactions, resulting in improved stability, as evidenced by its higher boiling point relative to LGO. This increased thermal stability is particularly advantageous for downstream applications involving elevated processing temperatures. Additionally, MHC is polar and protic and highly soluble in a wide range of solvents including water. Its broad solubility profile enhances its utility as a versatile intermediate in both aqueous and organic reaction media.

Beyond the carbonyl group's reactivity, the hydroxyl group also offers functionalisation opportunities, positioning MHC as a valuable platform molecule for the development of polymers and more complex derivatives. This dual functional group reactivity supports its potential for advanced material synthesis, pharmaceutical intermediate development, and the design of novel, bio-based functional molecules. By replacing fossil-based solvents and monomers, MHC contributes to decarbonisation efforts and supports the transition toward a circular economy. Its renewable origin and dual reactivity make it a promising building block for the development of sustainable materials with reduced environmental impact. Nevertheless, future work should explore strategies to accelerate the reaction kinetics at ambient temperatures to overcome the current limitation of slow conversion rates.

Supplementary Materials

The additional data and information can be downloaded at: https://media.sciltp.com/articles/others/250728092719 9177/ESIforMHCDraftforRenewableChemistry.pdf. Figure S1: IR spectra of LGO and MHC. Figure S2: 1H NMR spectrum of MHC, Figure S3: MS of MHC prepared from H_2O (top) and D_2O (bottom) Figure S4: The difference between ^1H NMR spectra of MHC prepared from H_2O and D_2O, Figure S5: Proton coupling on C3, Figure S6: IR spectra of MHC in different water sources and production methods, Figure S7: IR spectra for MHC prepared in different temperatures, Figure S8: ^{13}C NMR spectra for MHC prepared in different temperatures, Figure S9: UV-Vis spectra of Reichardt's dye in the presence of MHC (deconvoluted bands), Figure S10: IR spectrum of 10% MHC in D_2O shows no vibration band for the ketone, Figure S11: STA data showing MHC has higher boiling point than both Cyrene and LGO, Figure S12: EtOAc extraction method, Figure S13: ^1H COSY NMR spectrum for MHC in $CDCl_3$. The MHC was produced from LGO dissolved in H_2O, Figure S14: 2D ^1H+^{13}C HSQC NMR spectrum for MHC in $CDCl_3$. The MHC was produced from LGO dissolved in H_2O, Figure S15: DSC for MHC, Figure S16: 3D modelling using COSMO to identify the intramolecular H-bonding for MHC, in different electronic configurations, Table S1: Mass fragments of MHC, Table S2: CHN analysis, Table S3: ^{13}C NMR spectroscopy assessment for MHC, Table S4: ^1H NMR spectroscopy assessment for MHC, Table S5: Integration results for protons on C3 of the MHC prepared from H_2O, Table S6: Integration results for protons on C3 of the MHC prepared from D_2O, Table S7: Integration results for protons on C3 of the MHC prepared from H_2O, Table S8: Integration results for protons on C3 of the MHC prepared from D_2O, Table S9: Solubility of MHC in organic solvents. Scheme S1: LGO interaction with H_2O and D_2O, Scheme S2: The difference between LGO and MHC in water.

Author Contributions

M.A.; Formal Analysis, Investigation, Writing—original draft, C.R.M.; Formal Analysis, Supervision, Writing—review & editing, J.F.; Conceptualisation, Methodology, Supervision, Writing—review & editing J.H.C. Conceptualisation, Funding acquisition, Methodology, Supervision, Writing—review & editing. All authors have read and agreed to the published version of the manuscript.

Funding

This research was funded by the Joint Undertaking (BBI-JU) under grant agreement No 887674.

Institutional Review Board Statement

Not applicable.

Informed Consent Statement

Not applicable.

Data Availability Statement

We advocate for the sharing of research data by all authors contributing to publications in Scilight journals. In this section, authors may be asked to provide the raw data of their study together with the manuscript for editorial review and should be prepared to make the data publicly available if practicable. In any event, authors should ensure accessibility of such data to other competent professionals for at least 10 years after publication (preferably via an institutional or subject-based data repository or other data center), provided that the confidentiality of the participants can be protected and legal rights concerning proprietary data do not preclude their release. In instances where novel data were not generated or data remains inaccessible due to privacy or ethical considerations, a clear statement outlining these circumstances is mandatory.

Conflicts of Interest

The authors declare no conflict of interest.

Acknowledgements

The JU receives support from the European Union's Horizon 2020 research and innovation programme and the Bio Based Industries Consortium. The authors also would like to thank Circa Group for providing the LGO and the Saudi Cultural Bureau for the scholarship fund.

References

1. Fankhauser, S.; Smith, S.M.; Allen, M.; et al. The meaning of net zero and how to get it right. *Nat. Clim. Chang.* **2022**, *12*, 15–21.
2. Christopher, S.; Vikram, M.; Bakli, C.; et al. Renewable energy potential towards attainment of net-zero energy buildings status–A critical review. *J. Clean. Prod.* **2023**, *405*, 136942.
3. Bonsu, N.O. Towards a circular and low-carbon economy: Insights from the transitioning to electric vehicles and net zero economy. *J. Clean. Prod.* **2020**, *256*, 120659.
4. Ritchie, H. Sector by Sector: Where Do Global Greenhouse Gas Emissions Come from? Available online: https://ourworldindata.org/ghg-emissions-by-sector (accessed on 11 June 2025).
5. Griffiths, S.; Sovacool, B.K.; Iskandarova, M.; et al. Bridging the gap between defossilization and decarbonization to achieve net-zero industry. *Environ. Res. Lett.* **2025**, 20, 024063.
6. Sparks, J.; Scaldaferri, C.; Welfle, A.; et al. *Carbon for Chemicals: How Can Biomass Contribute to the Defossilisation of the Chemicals Sector?* University of Manchester: Manchester, UK, 2024.
7. Attard, T.M.; Clark, J.H.; McElroy, C.R. Recent developments in key biorefinery areas. *Curr. Opin. Green Sustain. Chem.* **2020**, *21*, 64–74.
8. Clark, J.H. Green biorefinery technologies based on waste biomass. *Green Chem.* **2019**, *21*, 1168–1170.
9. Awasthi, M.K.; Sindhu, R.; Sirohi, R.; et al. Agricultural waste biorefinery development towards circular bioeconomy. *Renew. Sustain. Energy Rev.* **2022**, *158*, 112122.
10. Van den Bosch, S.; Schutyser, W.; Vanholme, R.; et al. Reductive lignocellulose fractionation into soluble lignin-derived phenolic monomers and dimers and processable carbohydrate pulps. *Energy Environ. Sci.* **2015**, *8*, 1748–1763.
11. Mak, T.M.; Xiong, X.; Tsang, D.C.; et al. Sustainable food waste management towards circular bioeconomy: Policy review, limitations and opportunities. *Bioresour. Technol.* **2020**, *297*, 122497.
12. Govindasamy, G.; Jaya Balaji, P.K. Configuring municipal solid and liquid waste treatment plants into bio-refinery to achieve sustainable development goals. *J. Mater. Cycles Waste Manag.* **2025**, 27, 2016–2031.
13. Sherwood, J. The significance of biomass in a circular economy. *Bioresour. Technol.* **2020**, *300*, 122755.
14. Farmer, T.J.; Mascal, M. Platform molecules. *Introd. Chem. Biomass* **2015**, 89–155. https://doi.org/10.1002/9781118714478.ch4.
15. Tian, C.; Dorakhan, R.; Wicks, J.; et al. Progress and roadmap for electro-privileged transformations of bio-derived molecules. *Nat. Catal.* **2024**, *7*, 350–360.
16. Yong, K.J.; Wu, T.Y.; Lee, C.B.T.L.; et al. Furfural production from biomass residues: Current technologies, challenges and future prospects. *Biomass Bioenergy* **2022**, *161*, 106458.
17. Rackemann, D.W.; Doherty, W.O. The conversion of lignocellulosics to levulinic acid. *Biofuels Bioprod. Biorefining* **2011**, *5*, 198–214.

18. Prete, P.; Cespi, D.; Passarini, F.; et al. Glycidol syntheses and valorizations: Boosting the glycerol biorefinery. *Curr. Opin. Green Sustain. Chem.* **2022**, *35*, 100624.
19. Klement, T.; Büchs, J. Itaconic acid–A biotechnological process in change. *Bioresour. Technol.* **2013**, *135*, 422–431.
20. Allais, F. Total syntheses and production pathways of levoglucosenone, a highly valuable chiral chemical platform for the chemical industry. *Curr. Opin. Green Sustain. Chem.* **2023**, *40*, 100744.
21. Gomez, M.; Quincoces, J.; Kuhla, B.; et al. *Synthesis of Push-Pull Derivatives of Levoglucosenone as Precursors of Annellated Pyranosides*; Taylor Francis: Oxford, UK, 1999.
22. Tsai, Y.-h.; Etichetti, C.M.B.; Cicetti, S.; et al. Design, synthesis and evaluation of novel levoglucosenone derivatives as promising anticancer agents. *Bioorg. Med. Chem. Lett.* **2020**, *30*, 127247.
23. Camp, J.E.; Greatrex, B.W. Levoglucosenone: Bio-based platform for drug discovery. *Front. Chem.* **2022**, *10*, 902239.
24. Sherwood, J.; Constantinou, A.; Moity, L.; et al. Dihydrolevoglucosenone (Cyrene) as a bio-based alternative for dipolar aprotic solvents. *Chem. Commun.* **2014**, *50*, 9650–9652.
25. Fan, J.; Budarin, V.; MacQuarrie, D.J.; et al. A new perspective in bio-refining: Levoglucosenone and cleaner lignin from waste biorefinery hydrolysis lignin by selective conversion of residual saccharides. *Energy Environ. Sci.* **2016**, *9*, 2571–2574.
26. Huang, X.; Kudo, S.; Asano, S.; et al. Improvement of levoglucosenone selectivity in liquid phase conversion of cellulose-derived anhydrosugar over solid acid catalysts. *Fuel Process. Technol.* **2021**, *212*, 106625.
27. Richardson, D.E.; Raverty, W.D. Predicted environmental effects from liquid emissions in the manufacture of levoglucosenone and Cyrene. *Appita: Technol. Innov. Manuf. Environ.* **2016**, *69*, 344–351.
28. Wilson, K.L.; Murray, J.; Jamieson, C.; et al. Cyrene as a bio-based solvent for HATU mediated amide coupling. *Org. Biomol. Chem.* **2018**, *16*, 2851–2854.
29. Camp, J.E. Bio-available solvent Cyrene: Synthesis, derivatization, and applications. *ChemSusChem* **2018**, *11*, 3048–3055.
30. Wilson, K.L.; Murray, J.; Jamieson, C.; et al. Cyrene as a bio-based solvent for the Suzuki–Miyaura cross-coupling. *Synlett* **2018**, *29*, 650–654.
31. ReSolute High Performing and Safe Solvent Derived from Celllulosic Feedstocks. Available online: https://www.cbe.europa.eu/projects/resolute (accessed on 17 June 2025).
32. Sheldon, R.A. Waste Valorization in a Sustainable Bio-Based Economy: The Road to Carbon Neutrality. *Chem. A Eur. J.* **2024**, *30*, e202402207.
33. Warne, C.M.; Fadlallah, S.; Whitwood, A.C.; et al. Levoglucosenone-derived synthesis of bio-based solvents and polyesters. *Green Chem. Lett. Rev.* **2023**, *16*, 2154573.
34. Stanfield, M.K.; Terry, R.S.; Smith, J.A.; et al. Levoglucosan and levoglucosenone as bio-based platforms for polymer synthesis. *Polym. Chem.* **2023**, *14*, 4949–4956.
35. Mouterde, L.M.; Allais, F.; Stewart, J.D. Enzymatic reduction of levoglucosenone by an alkene reductase (OYE 2.6): A sustainable metal-and dihydrogen-free access to the bio-based solvent Cyrene®. *Green Chem.* **2018**, *20*, 5528–5532.
36. Ma, X.; Liu, X.; Yates, P.; et al. Manipulating the enone moiety of levoglucosenone: 1, 3-Transposition reactions including ones leading to isolevoglucosenone. *Tetrahedron* **2018**, *74*, 5000–5011.
37. Sharipov, B.T.; Davydova, A.N.; Faizullina, L.K.; et al. Preparation of the diastereomerically pure 2S-hydroxy derivative of dihydrolevoglucosenone (cyrene). *Mendeleev Commun.* **2019**, *29*, 200–202.
38. Witczak, Z.J.; Kaplon, P.; Kolodziej, M. *Thiosugars VI: A Simple Stereoselective Approach to (1→3)-3-S-Thiodisaccharides from Levoglucosenone*; Springer: Berlin/Heidelberg, Germany, 2002.
39. Sharipov, B.T.; Davidova, A.N.; Ryabova, A.S.; et al. Synthesis and fungicidal activity of methylsulfanylmethyl ether derivatives of levoglucosenone. *Chem. Heterocycl. Compd.* **2019**, *55*, 31–37.
40. Witczak, Z.J.; Kaplon, P.; Kolodziej, M. Thiosugars VI: A Simple Stereoselective Approach to (1→3)-3-S-Thiodisaccharides from Levoglucosenone. In *Timely Research Perspectives in Carbohydrate Chemistry*; Springer: Berlin/Heidelberg, Germany, 2002; pp. 171–180.
41. Krishna, S.H.; Walker, T.W.; Dumesic, J.A.; et al. Kinetics of levoglucosenone isomerization. *ChemSusChem* **2017**, *10*, 129–138.
42. Diot-Néant, F.; Mouterde, L.; Couvreur, J.; et al. Green synthesis of 2-deoxy-D-ribonolactone from cellulose-derived levoglucosenone (LGO): A promising monomer for novel bio-based polyesters. *Eur. Polym. J.* **2021**, *159*, 110745.
43. Shafizadeh, F.; Furneaux, R.H.; Stevenson, T.T. Some reactions of levoglucosenone. *Carbohydr. Res.* **1979**, *71*, 169–191.
44. Mlostoń, G.; Urbaniak, K.; Palusiak, M.; et al. (3 + 2)-Cycloadditions of Levoglucosenone (LGO) with Fluorinated Nitrile Imines Derived from Trifluoroacetonitrile: An Experimental and Computational Study. *Molecules* **2023**, *28*, 7348.
45. Camp, J.; Greatrex, B. Levoglucosenone: Bio-based platform for drug discovery Front. *Chem* **2022**, *10*, 902239.
46. Plenert, A.C.; Mendez-Vega, E.; Sander, W. Micro-vs. macrosolvation in Reichardt's dyes. *J. Am. Chem. Soc.* **2021**, *143*, 13156–13166.
47. Jessop, P.G.; Jessop, D.A.; Fu, D.; et al. Solvatochromic parameters for solvents of interest in green chemistry. *Green Chem.* **2012**, *14*, 1245–1259.